UC Irvine
UC Irvine Previously Published Works

Title

Self-Assembled Monolayers on Pt(111): Molecular Packing Structure and Strain Effects Observed by Scanning Tunneling Microscopy

Permalink

https://escholarship.org/uc/item/2463v8jg

Journal

Journal of the American Chemical Society, 128(17)

ISSN

0002-7863

Authors

Lee, Sangyeob
Park, Jung
Ragan, Regina
et al.

Publication Date

2006-05-01

DOI

10.1021/ja058037c

Peer reviewed

Self-Assembled Monolayers on Pt(111): Molecular Packing Structure and Strain Effects Observed by Scanning Tunneling Microscopy

Sangyeob Lee,[†] Jung Park,[†] Regina Ragan,*,[†] Sehun Kim,[‡] Zonghoon Lee,[§] Do Kyung Lim,[‡] Douglas A. A. Ohlberg,[||] and R. Stanley Williams[||]

Contribution from the Department of Chemical Engineering and Materials Science, University of California, Irvine, California 92697, Department of Chemistry, Korea Advanced Institute of Science and Technology, 373-1 Guseong-dong, Yuseong-gu, Daejeon 305-701, Korea, National Center for Electron Microscopy, Lawrence Berkeley National Lab, MS 72-150, 1 Cyclotron Road, Berkeley, California 94720, and Quantum Science Research Group, Hewlett-Packard Laboratories, MS 1123, 1501 Page Mill Road, Palo Alto, California 94303

Received December 7, 2005; E-mail: rragan@uci.edu

Abstract: Self-assembled monolayers (SAMs) of octanethiol and benzeneethanethiol were deposited on clean Pt(111) surfaces in ultrahigh vacuum (UHV). Highly resolved images of these SAMs produced by an in situ scanning tunneling microscope (STM) showed that both systems organize into a super-structure mosaic of domains of locally ordered, closely packed molecules. Analysis of the STM images indicated a $(\sqrt{3} \times \sqrt{3})R30°$ unit cell for the octanethiol SAMs and a $4(\sqrt{3} \times \sqrt{3})R30°$ periodicity based on 2×2 basic molecular packing for the benzeneethanethiol SAMs under the coverage conditions investigated. SAMs on Pt(111) exhibited differences in molecular packing and a lower density of disordered regions than SAMs on Au(111). Electron transport measurements were performed using scanning tunneling spectroscopy. Benzeneethanethiol/Pt(111) junctions exhibited a higher conductance than octanethiol/Pt(111) junctions.

Introduction

Molecular/metal interfaces are of technological interest as key components in innovative devices that will impact electronic, sensing, and catalytic applications. Metal/molecule/silicon nanowire junctions have potential applications as highly dense, low cost logic and memory devices in a defect-tolerant cross bar architecture.[1-3] Organically functionalized, metal nanocrystal surfaces can detect biological molecules such as DNA and proteins in femtomolar quantities and thus have great potential as highly sensitive, biomolecular detection devices.[4] Unresolved issues associated with stability and reproducibility of these and other nanoscale devices must be addressed, however, before commercial products can be fabricated; thus, fundamental studies are necessary. Self-assembled monolayers (SAMs) on Au surfaces have been studied extensively since early 1980. In studies involving organosulfur compounds on Au(111), it was observed that thiols assemble into densely packed, monomolecular films arranged as a mosaic of domains that can be circumscribed by translational, rotational, tilt, or antiphase boundaries.[5-10] Scanning tunneling microscope (STM) images showed direct-space morphologies, and grazing incidence X-ray diffraction and He diffraction provided an estimate of the average domain size. These experimental techniques revealed that SAMs formed domains with preferred directions and vacancy islands along the domain boundaries.[11-17] Although Au is a well-studied system, ideal for a lab environment because of its ease of preparation and chemical inertness, it may not be desirable as a substrate material for SAMs because of a high density of vacancy island defects that arise after SAM formation. Other noble metals such as Pd[18] and Pt may be more commercially viable choices because of compatibility with CMOS processing. In the case of Pt, we have demonstrated the ability

---

[†] University of California.
[‡] Korea Advanced Institute of Science and Technology.
[§] Lawrence Berkeley National Lab.
[||] Hewlett-Packard Laboratories.

(1) Heath, R. J.; Kuekes, P. J.; Snider, G. S.; Williams, R. S. *Science* **1998**, *280*, 1716.
(2) DeHon, A. *IEEE Trans. Nanotechnol.* **2003**, *2*, 23.
(3) Jang, Y. H.; Kim, W. A.; Goddard, W. A.; Flood, A. H.; Laursen, B. W.; Tseng, H. R.; Sdoddart, J. R.; Choi, J. W.; Steuerman, D. W.; Delonno, E.; Heath, J. R. *J. Am. Chem. Soc.* **2005**, *127*, 1563.
(4) Cao, Y. W. C.; Jin, R.; Mirkin, C. A. *Science* **2002**, *297*, 1536.

(5) Nuzzo, R. G.; Allara, D. L. *J. Am. Chem. Soc.* **1983**, *105*, 4481.
(6) Porter, M. D.; Bright, T. B.; Allara, D. L.; Chudsey, C. E. D. *J. Am. Chem. Soc.* **1987**, *109*, 3559.
(7) Dubois, L. H.; Nuzzo, R. G. *Annu. Rev. Phys. Chem.* **1992**, *43*, 437.
(8) Yeganeh, M. S.; Dougal, S. M.; Polizzotti, R. S.; Rabinowitz, P. *Phys. Rev. Lett.* **1995**, *74*, 1811.
(9) Poirier, G. E. *Chem. Rev.* **1997**, *97*, 1117.
(10) Kluth, G. J.; Carraro, C.; Maboudian, R. *Phys. Rev. B* **1999**, *59*, 10449.
(11) Wang, Y. W.; Fan, L. J. *Langmuir* **2002**, *18*, 1157.
(12) Zamborini, F. P.; Crooks, R. M. *Langmuir* **1997**, *13*, 122.
(13) Delamarche, E.; Michel, B.; Kang, H.; Gerber, C. *Langmuir* **1994**, *10*, 4103.
(14) Delamarche, E.; Michel, B. *Thin Solid Films* **1996**, *273*, 54.
(15) Poirier, G. E.; Tarlov, M. J.; Rushmeier, H. E. *Langmuir* **1994**, *10*, 3383.
(16) McDermott, C. A.; McDermott, M. T.; Green, J. B.; Porter, M. D. *J. Phys. Chem.* **1995**, *99*, 13257.
(17) Fenter, P.; Eisenberger, P.; Liang, K. S. *Phys. Rev. Lett.* **1993**, *70*, 2447.
(18) Love, J. C.; Wolfe, D. B.; Haasch, R.; Chabinyc, M. L.; Paul, K. E.; Whitesides, G. M.; Nuzzo, R. G. *J. Am. Chem. Soc.* **2003**, *125*, 2597.

to prepare ultra-smooth surfaces on Si substrates using a template−strip fabrication method.[19] However, to the best of our knowledge, STM studies of the molecular packing structure of organosulfur molecules on Pt(111) are absent in the literature. We have, therefore, deposited benzeneethanethiol and octanethiol, each with two different doses, on clean, atomically flat Pt(111) surfaces in ultrahigh vacuum (UHV) to gain a fundamental understanding of SAM organization in this system. In this paper, we describe the molecular packing structures of benzeneethanethiol and octanethiol SAMs on Pt(111) and electron transport behavior across these organosulfur/Pt(111) junctions observed by STM. We compare these organosulfur/Pt(111) surfaces with structures observed in similar studies on Au(111) surfaces.

Experimental Section

Octanethiol and benzeneethanethiol monolayers were deposited on single-crystal Pt(111) substrates in an UHV system with a base pressure of 10^{-10} Torr. The single-crystal Pt(111) surface was prepared in the UHV chamber by first sputtering it at room temperature with a 1 kV, ca. 35 μA, Ar ion beam under dynamic flow conditions adjusted to maintain an Ar background pressure of 10^{-5} Torr. After sputtering, the Pt(111) substrate was annealed at 500 °C in an O_2 ambient of 10^{-8} Torr. The initial sputter regime was repeated and followed by an annealing in UHV at 500 °C. This process was iterated until STM imaging verified an atomically clean Pt(111) surface. Both organosulfur monolayers were deposited in the gas phase in a deposition chamber with a base pressure of 10^{-8} Torr that was connected to the UHV system. The vapor pressure of octanethiol and benzeneethanethiol during deposition was in the range of 10^{-5} to 10^{-6} Torr. Unless otherwise stated in the figure captions, the substrate temperature during deposition was room temperature. The UHV system also houses an Omicron VT-STM which we used to image changes in surface reconstruction with molecular coverage using a tungsten STM tip. We also performed scanning tunneling spectroscopy (STS) and compared conductance across octanethiol and benzeneethanethiol molecule/metal junctions. All measurements were carried out at room temperature.

Results and Discussion

Figure 1a,b shows 20 × 20 nm STM images of Pt(111) surfaces exposed to 30 langmuirs (L) of benzeneethanethiol and 60 L of octanethiol, respectively. Figure 1c shows a 10 × 10 nm high-resolution STM image of benzeneethanethiol monolayers on Pt(111) with an exposure of 30 L. Molecular packing directions are indicated by arrows. Benzeneethanethiol monolayers are packed along $\langle 1\bar{1}0 \rangle$, and octanethiol monolayers are packed along $\langle 1\bar{2}1 \rangle$ with respect to Pt(111). Each figure includes an inset in the lower right corner of a fast Fourier transform (FFT) of the image. The images and FFT patterns show that the SAMs adopt the hexagonal packing of the Pt(111) surface. The spacing between molecules in benzeneethanethiol and octanethiol was calculated as 0.55 ± 0.04 nm (1σ) and 0.47 ± 0.02 nm (1σ), respectively, as determined from the FFT patterns. When the nearest neighbor (nn) spacing of Pt (d) was calculated in a similar manner, a value of 0.27 ± 0.06 nm (1σ) was obtained. This is consistent with the nn spacing in the (111) plane for bulk Pt. On the basis of the FFT patterns and STM image analysis, octanethiol SAMs packed as ($\sqrt{3} \times \sqrt{3}$)R30° monolayers. Previous high-resolution STM studies showed that

alkanethiol SAMs exhibit a c(4 × 2) superlattice of a ($\sqrt{3} \times \sqrt{3}$)R30° basis densely packed monolayer on Au(111) at the saturation coverage.[20] Octanethiol monolayers on Pt(111) showed the same ($\sqrt{3} \times \sqrt{3}$)R30° packing structures but not the c(4 × 2) superlattice structure. The Pt(111) surface does not exhibit a surface reconstruction as does Au(111), and this explains the absence of the c(4 × 2) superlattice structure on Pt(111). In addition, Pt has a smaller lattice constant than Au, thus octanethiol molecules with a ($\sqrt{3} \times \sqrt{3}$)R30° packing structure on Pt(111) are more closely packed than those on Au(111). The observation of a more closely packed structure of octanethiol on Pt(111) vs Au(111) is in agreement with ellipsometry and reflection absorption infrared spectroscopy measurements that observe a tilting angle of less than 15° with respect to the surface normal on Pt(111)[21] vs 27°, the generally accepted tilting angle of alkanethiols on Au(111). However, benzeneethanethiol monolayers on Pt(111) exhibit a 2 × 2 packing basis along $\langle 1\bar{1}0 \rangle$. The peaks in the FFT pattern indicated by arrows in the insets of Figure 1a imply a $4\sqrt{3}d$ periodicity along $\langle 1\bar{2}1 \rangle$. These peaks have a measured period of 1.93 ± 0.07 nm (1σ). Figure 1c shows ridgelike features that are associated with a periodic modulation in intensity of the molecular features. In the STM image, four bright and two dark molecular features are observed along [10$\bar{1}$] and two bright and one dark features are observed along [01$\bar{1}$]. The alternating bright and dark molecular features repeat along [$\bar{2}$11] (this direction is indicated by an arrow in Figure 1c) and are consistent with the peak along $\langle 1\bar{2}1 \rangle$ in the FFT pattern. Although the molecular packing is along $\langle 1\bar{1}0 \rangle$, the dominant periodicity of the ridged feature is along $\langle 1\bar{2}1 \rangle$ for benzeneethanethiol/Pt(111). However, registry of this feature with the Pt(111) surface was not always exact. A periodicity along $\langle 1\bar{2}1 \rangle$ with a spacing of 1.922 nm can be described as a $4(\sqrt{3} \times \sqrt{3})$R30° structure. For clarity, Figure 1d shows a schematic representation of ridgelike features having a four $4(\sqrt{3} \times \sqrt{3})$R30° repeating unit (outlined in bold lines). The alternating bright and dark discrete molecular features (red and gray circles) along $\langle 1\bar{1}0 \rangle$ and the Pt surface atoms (white circles) are shown in Figure 1d. The FFT shown in the upper inset of Figure 1a shows the hexagonal symmetry of the ridgelike features observed on benzeneethanethiol/Pt(111) surfaces along $\langle 1\bar{2}1 \rangle$. A ridgelike structure based on alternating, discrete, molecular features was not observed in STM images of octanethiol monolayers on Pt(111). The 2 × 2 packing structure of benzeneethanethiol/Pt(111) is approximately 15% larger than the ($\sqrt{3} \times \sqrt{3}$)R30° packing structure of octanethiol/Pt(111). A schematic of both packing arrangements is illustrated in Figure S1 in the Supporting Information. Strong steric interactions between molecules likely occur in SAMs of deposited benzeneethanethiol, whereas such strong interactions would not be expected for octanethiol. Steric hindrance may be the cause of the more open molecular packing arrangement observed in the benzeneethanethiol vs octanethiol SAMs. Yet the more open structure can be associated with increased strain at the molecular/substrate interface, leading to a relief of strain within the domain itself. Strain at the benzeneethanethiol/Pt interface can locally be relieved by the formation of a ridged feature. This strain relief mechanism can be thought of in a manner similar to strain-

(19) Ragan, R.; Ohlberg, D. A. A.; Blackstock, J. J.; Kim, S.; Williams, R. S. *J. Phys. Chem. B* **2004**, *108*, 20187.

(20) Poirier, G. E.; Tarlov, M. J. *Langmuir* **1994**, *10*, 2853.
(21) Li, Z.; Chang, S. C.; Williams, R. S. *Langmuir* **2003**, *19*, 6744.
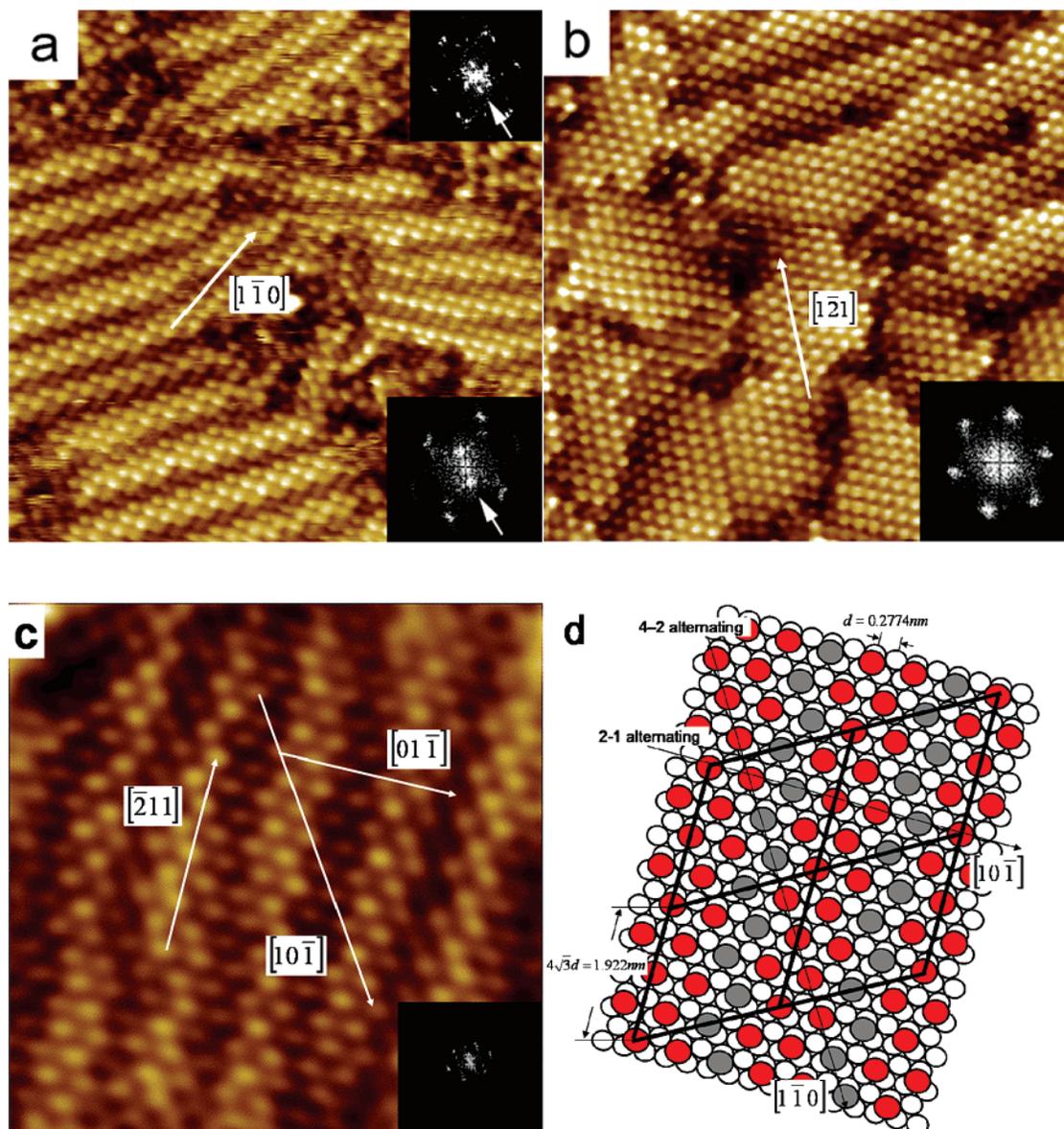
Figure 1. 20 × 20 nm STM images of Pt(111) dosed with (a) 30 L of benzeneethanethiol and (b) 60 L of octanethiol with the sample heated to 56 °C during deposition. (c) 10 × 10 nm high-resolution STM image of the 30 L benzeneethanethiol-dosed surface. Insets show FFT patterns. (d) Schematic diagram depicting the arrangement of benzeneethanethiol monolayers on the Pt(111) lattice. (Sample bias during image acquisition: (a) −1.482 V, (b) −0.582 V, (c) −0.492 V. Feedback current: (a) 223 pA, (b) 24.2 pA, (c) 162 pA.)

induced nanowire formation. Strain energy is associated with differences in preferred intermolecular (atomic) spacing between overlayers and the substrate at the interface. This excess strain energy in the vicinity of the interface can be minimized by forming a surface undulation in the overlayer.[22] The molecules assemble with a preferred intermolecular spacing, yet they can only assemble with this spacing and keep registry with the Pt(111) surface up to a critical width[23] defined by the mismatch between the preferred intermolecular spacing and the nearest neighbor distance on Pt(111). Once this width is exceeded, the benzeneethanethiol molecules may twist or tilt to relieve strain, thus leading to this periodic ridged feature. Twisting or tilting leading to a lower topographic height is a possible explanation for the darker molecular features in Figure 1c, although local

electronic structure is also a possible factor. Strain-induced ordering has a preferred width with a distribution around this width, thus this explanation is consistent with regions observed in the STM image of Figure 1c that deviate from the $4(\sqrt{3} \times \sqrt{3})$R30° repeating unit. The interaction between neighboring octanethiol molecules is presumably weaker than that between benzeneethanethiol molecules, enabling the molecules to pack uniformly inside domains leading to relatively uniform intensity in the domains of STM images.

Another difference between the FFT patterns (shown as insets in the lower right corner) of the two SAMs in Figure 1a,b is that the benzeneethanethiol FFT has sharper split peaks whereas the octanethiol FFT has single diffuse peaks. For clarity, another FFT pattern that was taken from another image in which the split peaks are clearly resolvable is shown as an inset in the upper right corner of Figure 1a. To understand the peak splitting observed for the FFT patterns of benzeneethanethiol, we refer

(22) Chen, Y.; Ohlberg, D. A. A.; Medeiros-Ribeiro, G.; Chang, Y. A.; Williams, R. S. *Appl. Phys. Lett.* **2000**, *76*, 4004.
(23) Ragan, R.; Chen, Y.; Ohlberg, D. A. A.; Medeiros-Ribeiro, G.; Williams, R. S. *J. Cryst. Growth* **2003**, *251*, 657.
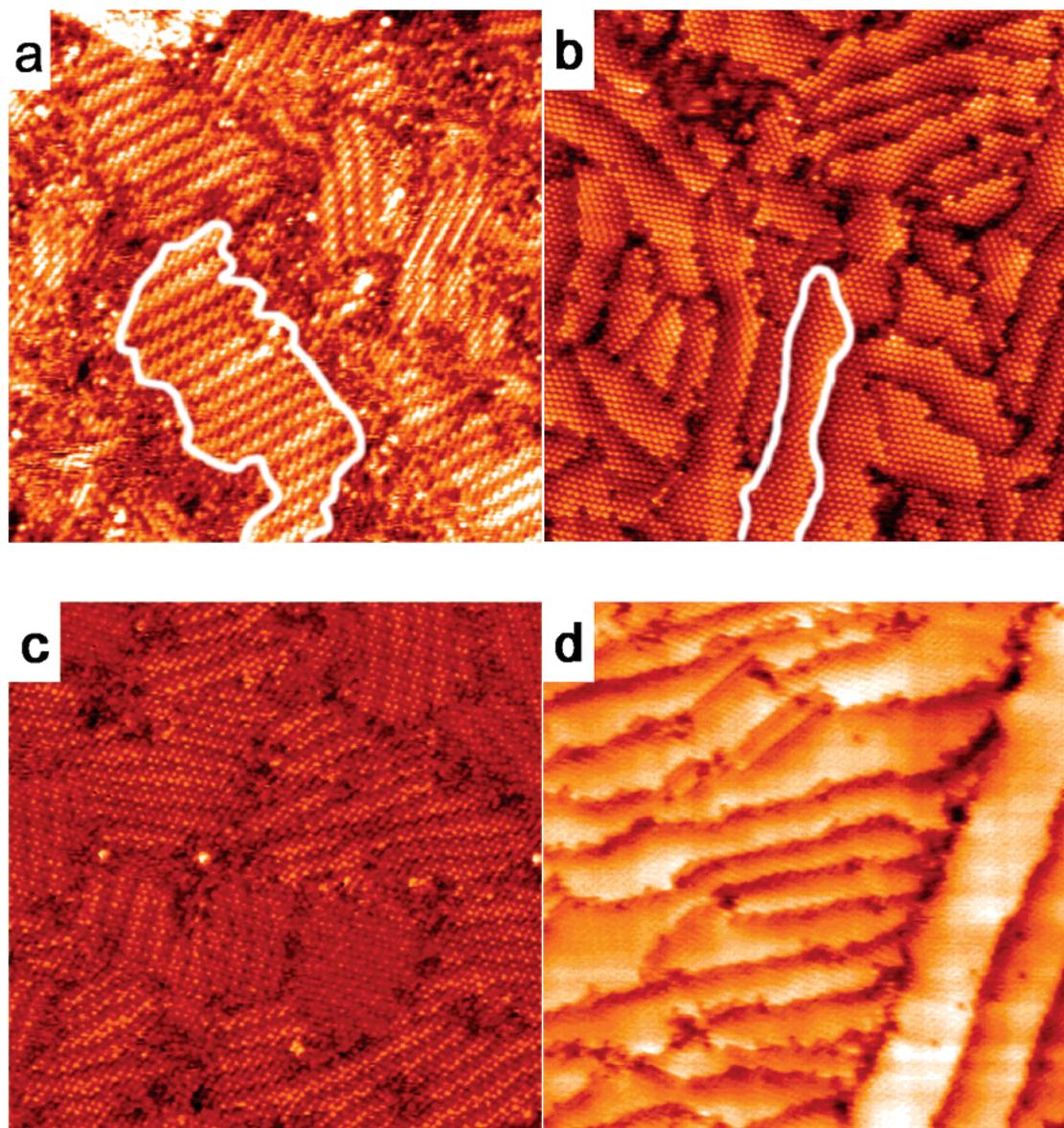
Figure 2. 40 × 40 nm STM images of Pt(111) dosed with (a) 30 L of benzeneethanethiol, (b) 60 L of octanethiol with the sample heated to 56 °C during deposition, (c) 6400 L of benzeneethanethiol, and (d) 4800 L of octanethiol monolayers. (Sample bias during image acquisition: (a) −1.544 V, (b) −0.582 V, (c) −0.839 V, (d) −1.115 V. Feedback current: (a) 772 pA, (b) 24.2 pA, (c) 203 pA, (d) 114 pA.)

to the FFT of Figure 1c that shows a single peak. The difference between Figure 1a and Figure 1c is that in Figure 1a multiple domain orientations are found, and in Figure 1c only a single orientation is found. This small domain rotation is further evidence that benzeneethanethiol molecules do not have exact registry with respect to the Pt(111) surface possibly because of strain relaxation. The peak broadening observed in the FFT of octanethiol is simply attributed to a smaller domain size of octanethiol vs benzeneethanethiol.

Figure 2 shows 40 × 40 nm STM images of these two organosulfur SAMs on Pt(111), each at two different coverages. Figure 2a,b shows benzeneethanethiol and octanethiol monolayers deposited on Pt(111) at 30 and 60 L, respectively, and Figure 2c,d shows benzeneethanethiol and octanethiol monolayers deposited on Pt(111) at 6400 and 4800 L, respectively. Domains in octanethiol monolayers are oriented along $\langle 1\bar{2}1 \rangle$ with respect to Pt(111). Benzeneethanethiol monolayers also show 3-fold mosaic domain structures mainly oriented along

$\langle 1\bar{1}0 \rangle$ directions, although $\langle 1\bar{2}1 \rangle$ domain orientations were also found. Translational and rotational domain boundary registries were found in both monolayers. The domain boundaries are highlighted in Figure 2a,b. The mean equivalent diameters of domains of benzeneethanethiol and octanethiol are 8.89 and 5.08 nm at the lower coverage and 8.81 and 7.22 nm at the higher coverage, respectively. The largest equivalent diameter of domains investigated at the lower coverage were 9.86 nm in octanethiol and 12.51 nm in benzeneethanethiol, and those investigated at the higher coverage were 11.64 nm in octanethiol and 12.42 nm in benzeneethanethiol. In comparison, the domain size of SAMs on Au(111) ranges from 5 to 15 nm.[9] Domain sizes of octanethiol on Pt(111) increase as coverage increases, whereas that of benzeneethanethiol does not change significantly. The mean domain size of benzeneethanethiol at both coverages investigated did not change with coverage and was higher than that of octanethiol. We attribute the larger observed domain size to the fact that benzeneethanethiol has a strain

Table 1. Characteristics of SAMs on Pt(111) and Au(111) Surfaces

	dodecanethiol/Au(111)	octanethiol/Pt(111)	benzeneethanethiol/Pt(111)
nn spacing of substrate	0.2884 nm	0.2774 nm	0.2774 nm
molecular packing	$(\sqrt{3} \times \sqrt{3})$R30°	$(\sqrt{3} \times \sqrt{3})$R30°	(2×2)
surface defect density	15%	2.19%	5.86%
mean equivalent diameter of surface defect	4.3 nm	0.85 nm	1.03 nm
molecular packing characteristic	30° tilted[a] c(4 × 2)superlattice	<15° tilted[b] homogeneous coverage	4$(\sqrt{3} \times \sqrt{3})$R30° ridgelike features

[a] From ref 20. [b] From ref 21.

relaxation mechanism within the domain. In the case of octanethiol, strain relaxation only occurs along the domain boundaries.

In both cases of organosulfur SAMs on Pt(111), domains are separated by molecular-scale domain boundaries. Disordered regions are sometimes observed along the domain boundaries. Image processing analysis of 40 × 40 nm STM images yielded values for the average equivalent diameter and the fraction of total scan area occupied by the disordered regions. Figures S2, S3, and S4 in the Supporting Information highlight the disordered regions that were used in the calculations of these values. The calculated fraction occupied by the disordered area for benzeneethanethiol/Pt(111) is 5.86% and 0.72%, and the average equivalent diameter of the disordered area is calculated as 1.03 and 0.74 nm for coverages of 30 and 6400 L, respectively. For octanethiol/Pt(111), the calculated fraction occupied by the disordered area is 2.19% and 1.10% and the average equivalent diameter of the disordered area is calculated as 0.85 and 0.82 nm for coverages of 60 and 4800 L, respectively. Disordered regions decrease as exposure increases. Image processing analysis of an STM image of dodecanethiol/Au(111) taken from ref 24 yielded a disordered area fraction of 15%, and the average equivalent diameter of vacancy islands is calculated as 4.3 nm. In further contrast between Au and Pt, the disordered regions in SAMs on Pt(111) have feature heights of approximately 1 Å, smaller than a Pt(111) single-atom step height (2.27 Å); SAMs on Au(111) exhibit a high density of vacancy islands that have a depth consistent with a Au(111) single-atom step height.[25,26] We only observed disordered regions with feature heights of less than 2.27 Å and thus do not see any evidence for vacancy island formation after organosulfur SAM deposition on Pt(111). The disordered region with feature heights of less than the Pt(111) single-atom step height can be associated with disorder in the packing arrangement at domain boundaries. The Pt(111) substrate surface is atomically flat, having corrugation heights of 0.02 nm on a single terrace. The measured nn atomic spacing on the Pt(111) surface of 0.27 ± 0.06 nm (1σ) and the absence of a surface reconstruction that differs from the bulk are in agreement with our previous measurement of the nn spacing of 0.25 ± 0.03 nm as determined from a FFT pattern of an STM image.[19] In comparison, the reconstructed Au(111) surface is characterized by a 4.3% uniaxial lateral contraction relative to the bulk layers.[27] This contraction causes an alternating stacking arrangement, the so-called herringbone pattern. Vacancy islands on Au(111) have been attributed to surface relaxation during

SAM deposition.[28] On the basis of the absence of a surface reconstruction different from the bulk on a clean Pt(111) surface and a lower atomic mobility of Pt vs Au, we do not expect significant surface relaxation of Pt atoms on Pt(111) surfaces. Overall, octanethiol SAMs on Pt(111) have fewer defects and more homogeneous coverage than benzeneethanethiol SAMs on Pt(111) and alkanethiol SAMs on Au(111). Octanethiol molecules packed in a $(\sqrt{3} \times \sqrt{3})$R30° unit cell are more tightly packed and thereby oriented closer to the surface normal on Pt(111) than on Au(111) surfaces because of the smaller lattice constant of Pt vs Au and are more closely packed than benzeneethanethiol molecules in a (2×2) packing structure on Pt(111); thus, domain walls of octanethiol SAMs on Pt(111) are expected to be thinner leading to a lower disordered area from domain boundaries. Yet, the defect density of both SAMs of octanethiol and benzeneethanethiol on Pt(111) differed only by a factor of 2, whereas when compared to SAMs on Au(111), the defect density was significantly higher. SAMs on Pt(111) had no observable vacancy islands, and therefore, both SAMs had a significantly lower defect density than SAMs on Au(111). For clarity, Table 1 summarizes the characteristics of SAMs on Pt(111) and Au(111) surfaces.

Electron transport data of benzeneethanethiol/Pt(111) and octanethiol/Pt(111) junctions at a lower coverage are shown in Figure 3a. Figure 3b shows the normalized differential conductance curves of octanethiol/Pt(111) and benzeneethanethiol/Pt(111) junctions. *I*−*V* responses are different in the two monolayers. The octanethiol/Pt(111) junction has zero conductance at zero volts and exhibits a gap. For the benzeneethanethiol/Pt(111) junction, there is a finite conductance at zero volts and thus no apparent gap. The benzeneethanethiol/Pt(111) junction exhibits metallic behavior. Although electron transport across molecular/metal junctions in SAMs is not completely understood, it is generally accepted that conduction through molecular/metal junctions is dependent on the molecule as well as on the metal electrode.[29−32] An increased conductivity of a phenylene ethynylene molecule/Au(111) junction, relative to an alkanethiolate molecule/Au(111) junction, was reported. The report attributes this increase to the conjugated molecular structure which facilitates electron transport through a delocalized p-orbital structure.[33] Our STS data from two different molecular systems can be understood in a similar manner. The

(24) Schonenberger, C.; Jorritsma, J.; Sondag-Huethorst, J. A. M.; Fokkink, L. G. J. *J. Phys. Chem.* **1995**, *99*, 3259.
(25) Poirier, G. E. *Langmuir* **1997**, *13*, 2019.
(26) Dishner, M. H.; Hemminger, J. C.; Feher, J. F. *Langmuir* **1997**, *13*, 2318.
(27) Sandy, A. R.; Mochrie, S. G. J.; Zehner, D. M.; Huang, K. G.; Gibbs, D. *Phys. Rev. B* **1991**, *43*, 4667.

(28) Love, J. C.; Estroff, L. A.; Kriebel, J. K.; Nuzzo, R. G.; Whitesides, G. M. *Chem. Rev.* **2005**, *105*, 1103.
(29) Salomon, A.; Cahen, D.; Lindsay, S.; Tomfohr, J.; Engelkes, V. B.; Frisbie, C. D. *Adv. Mater.* **2003**, *15*, 1881.
(30) Wang, W.; Lee, T.; Reed, M. A. *Rep. Prog. Phys.* **2005**, *68*, 523.
(31) Stewart, D. R.; Ohlberg, D. A. A.; Beck, P. A.; Chen, Y.; Williams, R. S.; Jeppesen, J. O.; Nielsen, K. A.; Stoddart, J. F. *Nano Lett.* **2004**, *4*, 133.
(32) Lau, C. N.; Stewart, D. R.; Williams, R. S.; Bockrath, M. *Nano Lett.* **2004**, *4*, 569.
(33) Cygan, M. T.; Dunbar, T. D.; Arnold, J. J.; Bumm, L. A.; Shedlock, N. F.; Burgin, T. P.; Jones, L.; Allara, D. L.; Tour, J. M.; Weiss, P. S. *J. Am. Chem. Soc.* **1998**, *120*, 2721.
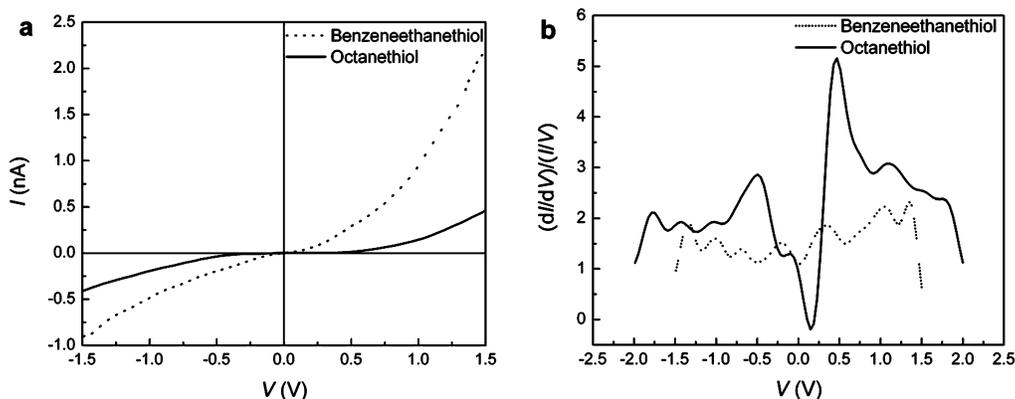
Figure 3. (a) $I-V$ curves obtained using scanning tunneling spectroscopy for benzeneethanethiol/Pt junctions (dashed curve) and octanethiol/Pt junctions (solid curve). (b) Normalized differential conductance for 30 L of benzeneethanethiol (dashed curve) and 60 L of octanethiol (solid curve) SAMs.

benzeneethanethiol/Pt(111) junction exhibits higher conductance at all voltages than the octanethiol/Pt(111) junction. A higher conductivity across benzeneethanethiol/Pt(111) junctions vs octanethiol/Pt(111) junctions can be attributed to the fact that the benzeneethanethiol molecule has conjugated bonds. The conjugated bonds allow for a uniformly distributed density of states. Further STM work is geared toward studying the effect of molecular orientation on electron transport across organosulfur molecule/Pt(111) junctions.

Conclusion

We deposited SAMs of octanethiol and benzeneethanethiol on Pt(111) surfaces, and STM images and FFT patterns indicate a molecular packing arrangement in a $(\sqrt{3} \times \sqrt{3})R30°$ structure for octanethiol SAMs and a $4(\sqrt{3} \times \sqrt{3})R30°$ periodicity based on 2×2 basic molecular packing for benzeneethanethiol SAMs at the coverages investigated. The observed different molecular packing structures of the two SAMs on Pt(111) can be explained by strain relaxation processes during benzeneethanethiol deposition that lead to a ridgelike feature with $4(\sqrt{3} \times \sqrt{3})R30°$ periodicity. Strain is likely caused by steric hindrance and by the difference between the interatomic spacing of Pt and the preferred benzeneethanethiol intermolecular spacing in the SAM. On a larger scale, SAMs on Pt(111) are composed of a mosaic of domains with preferred orientations and separated by molecular-width domain boundaries. The mean domain sizes measured for benzeneethanethiol and octanethiol monolayers were 8.81 and 7.22 nm, respectively, at the higher coverages investigated. Deposition on ultra-flat template-stripped Pt surfaces will be investigated to increase the domain size. Although STM images of SAMs on Pt(111) revealed disordered regions along domain boundaries, vacancy islands such as those found in SAMs on Au(111) were not observed. Statistical analysis of STM images showed that surface defects were of smaller size and lower density on the Pt(111) surface than those on the Au(111) surface. STS measurements demonstrated that current conductance through benzeneethanethiol monolayers was higher than that through octanethiol monolayers as expected. In summary, SAMs on Pt(111) showed more ordered packing than SAMs on Au(111). Thus, we demonstrate that Pt(111) is a suitable substrate for the deposition of well-ordered SAMs and STS can be used to measure electron transport of molecular/Pt junctions at the nanoscale. Highly ordered SAMs with low surface defect density are requisite for metal/molecule/metal device components having a high yield of functioning devices.

Supporting Information Available: A schematic representation of $(\sqrt{3} \times \sqrt{3})R30°$ packing and 2×2 packing. Image processing analysis of STM images used to calculate the area density of the disordered surface area of benzeneethanethiol/Pt(111), octanethiol/Pt(111), and dodecanethiol/Au(111). This material is available free of charge via the Internet at http://pubs.acs.org.

JA058037C